Neurotrophic signaling deficiency exacerbates environmental risks for Alzheimer's disease pathogenesis

Zhourui Wu[a,b,c], Chun Chen[a], Seong Su Kang[a], Xia Liu[a], Xiaohuan Gu[d], Shan Ping Yu[d], C Dirk Keene[e], Liming Cheng[b,c,1], and Keqiang Ye[a,1]

[a]Department of Pathology and Laboratory Medicine, Emory University School of Medicine, Atlanta, GA 30322; [b]Division of Spine, Department of Orthopedics, Tongji Hospital Affiliated to Tongji University School of Medicine, Shanghai 200065, China; [c]Key Laboratory of Spine and Spinal Cord Injury Repair and Regeneration, Ministry of Education, Shanghai 200072, China; [d]Department of Anesthesiology, Emory University School of Medicine, Atlanta, GA 30322; and [e]Department of Pathology, University of Washington School of Medicine, Seattle, WA 98104

Edited by Solomon H. Snyder, Johns Hopkins University School of Medicine, Baltimore, MD, and approved March 24, 2021 (received for review January 17, 2021)

The molecular mechanism of Alzheimer's disease (AD) pathogenesis remains obscure. Life and/or environmental events, such as traumatic brain injury (TBI), high-fat diet (HFD), and chronic cerebral hypoperfusion (CCH), are proposed exogenous risk factors for AD. BDNF/TrkB, an essential neurotrophic signaling for synaptic plasticity and neuronal survival, are reduced in the aged brain and in AD patients. Here, we show that environmental factors activate C/EBPβ, an inflammatory transcription factor, which subsequently up-regulates δ-secretase that simultaneously cleaves both APP and Tau, triggering AD neuropathological changes. These adverse effects are additively exacerbated in $BDNF^{+/-}$ or $TrkB^{+/-}$ mice. Strikingly, TBI provokes both senile plaque deposit and neurofibrillary tangles (NFT) formation in $TrkB^{+/-}$ mice, associated with augmented neuroinflammation and extensive neuronal loss, leading to cognitive deficits. Depletion of C/EBPβ inhibits TBI-induced AD-like pathologies in these mice. Remarkably, amyloid aggregates and NFT are tempospatially distributed in $TrkB^{+/-}$ mice brains after TBI, providing insight into their spreading in the progression of AD-like pathologies. Hence, our study revealed the roles of exogenous (TBI, HFD, and CCH) and endogenous (TrkB/BDNF) risk factors in the onset of AD-associated pathologies.

sporadic Alzheimer's disease | C/EBPβ | δ-secretase | risk factors | AEP

Alzheimer's disease (AD) is a chronic and progressive neurodegenerative disease with age as its major risk factor. AD is the most common form of dementia and is characterized by widespread extracellular senile plaques, mainly composed of amyloid-β (Aβ) peptides and intraneuronal neurofibrillary tangles, predominantly consisting of truncated and hyperphosphorylated Tau (1). Familial AD is attributed to mutations in one of three genes: APP (amyloid precursor protein), PS (Presenilin) 1, and PS2. Less than 5% of AD cases have an autosomal-dominant genetic etiology, however, and the etiology and pathogenesis of sporadic AD is complex and uncertain. There is currently no animal model that accurately recapitulates sporadic AD, yet an overwhelming emphasis and investment has been placed on transgenic AD models to understand AD pathogenesis. The precise cause of sporadic AD remains elusive, but several environmental risk factors (i.e., traumatic brain injury [TBI], diabetes, and chronic cerebral hypotension [CCH]) have been described as risk factors for the disease. TBI is linked to earlier onset of AD (2), and some studies claim that AD risk is directly correlated with TBI severity (3, 4). TBI causes axonal transport deficits, resulting in accumulation of various organelles and proteins [i.e., neurofilaments and APP (5)]. Tau has been linked to axonal damage following TBI (6, 7). Specifically, the presence of cleaved tau in cerebrospinal fluid (CSF) is a highly sensitive indicator of axonal injury (8) and may be a reliable biomarker for neuronal injury in human TBI and experimental animal models (9). Similarly, type 2 diabetes increases the risk of late-onset AD (10, 11). AD has been called "type 3 diabetes," with features of both insulin deficiency and insulin resistance in the brain. This is supported by a body of evidence such as decreased level of insulin and its receptor in the brain, de-sensitization of insulin receptor, and decreased levels and impaired functions of downstream components of the insulin signaling pathway in the AD brain (12–15). Furthermore, Aβ oligomers bind to brain insulin receptors and induce the redistribution of the receptors from the membrane to the cytoplasm, leading to impaired insulin signaling (16). Epidemiological studies associate cerebral ischemia with increased incidence of AD (17, 18). Imaging studies suggest that reduced cerebral blood flow appears early and precedes the onset of AD pathology, and the level of reduction is correlated with the severity of dementia (19). Clinically, patients with AD and a history of cerebrovascular disease, which leads to CCH, have a more rapid progression of dementia (20). Experimentally, CCH exacerbates AD-like pathology in young APPswe/PS1 mice by affecting the ability of microglia to naturally eliminate Aβ from the brain parenchyma (21). Spatial memory is significantly impaired 8 wk after CCH, and Aβ40 is increased in the CCH group (22).

Significance

The molecular mechanisms accounting for the environmental risk factor stimulation of Alzheimer's disease (AD) pathogenesis including traumatic brain injury, diabetes, and chronic cerebral hypoperfusion remain unclear. The BDNF/TrkB signaling pathway plays a critical role in neuronal synaptic plasticity and neuronal survival. Since the BDNF/TrkB pathway is reduced during aging and in AD human brains, we hypothesize that the crosstalk between these risk factors and BDNF/TrkB deficiency may mediate AD pathologies. Our previous studies establish that the C/EBPβ/δ-secretase pathway plays a pivotal role in triggering the major AD pathologies. Therefore, in the current report, we provide extensive evidence demonstrating that BDNF/TrkB reduction regulates this pathway activation under various risk factors, mediating Aβ and Tau pathology spreading in the brain.

Author contributions: K.Y. designed research; Z.W., C.C., S.S.K., X.L., X.G., and S.P.Y. performed research; C.D.K. contributed new reagents/analytic tools; Z.W., X.G., S.P.Y., L.C., and K.Y. analyzed data; and C.D.K. and K.Y. wrote the paper.

The authors declare no competing interest.

This article is a PNAS Direct Submission.

[1]To whom correspondence may be addressed. Email: limingcheng@tongji.edu.cn or kye@emory.edu.

This article contains supporting information online at https://www.pnas.org/lookup/suppl/doi:10.1073/pnas.2100986118/-/DCSupplemental.

Published June 17, 2021.

Neurotrophins are growth factors that regulate neuronal development, differentiation, and survival in the central and peripheral nervous system and mediate effects through specific cell surface receptors. Brain-derived neurotrophic factor (BDNF) binds to TrkB receptors and triggers activation of numerous signaling cascades, which play critical roles in neuronal plasticity, survival, neurogenesis, etc. The BDNF/TrkB signaling pathway is essential for long-term potentiation (LTP) induction and maintenance and long-term memory (23–25). Expressions of BDNF and TrkB are reduced in AD patients (26, 27). Furthermore, neurofibrillary tangles and BDNF immunoreactivity do not colocalize (neurons containing NFT lack BDNF immunoreactivity and vice versa) (28). BDNF administration increases learning and memory of cognitively impaired animals (29), and studies in experimental AD models show that BDNF has a neuroprotective effect against β-amyloid toxicity (30). Thus, the BDNF/TrkB signaling pathway may have a protective role against AD pathogenesis.

Recently, we reported that the δ-secretase, asparagine endopeptidase (AEP, gene name *LGMN*), cleaves both APP and Tau in an age-dependent manner in AD mouse models and in human AD brains. Its enzymatic activity and expression level escalate in an age-dependent manner (31, 32). It cleaves APP at both N373 and N585 residues in the ectodomain and facilitates Aβ production by decreasing the steric hindrance for BACE1. Depletion of δ-secretase significantly reduces Aβ production and senile plaque formation in 5XFAD mouse brain, leading to restoration of synaptic activity and cognitive functions (31). Additionally, δ-secretase cleaves Tau at N255 and N368 and abolishes its microtubule assembly activity, resulting in its aggregation and NFT formation. Notably, cleaved Tau 1 to 368 fragments are neurotoxic. Deletion of δ-secretase from Tau P301 mice reverses the synaptic plasticity defect and cognitive dysfunction (32). Hence, δ-secretase is necessary for AD onset and progression. Most recently, we reported that TBI activates δ-secretase, mediating AD pathologies by cleaving APP and Tau (33). Moreover, we identified that C/EBPβ (CCAAT-Enhancer Binding Protein beta), an age-dependent transcription factor, controls δ-secretase expression in brain (34). In addition to promoting the production of inflammatory mediators, C/EBP family members are themselves induced by the classical proinflammatory triad of IL-1, IL-6, and TNFα (35–38), all of which are significantly increased in pathologically impacted regions of the AD and PD brain (39, 40). Aβ and IL-6 additively increase C/EBPβ activity (41). Hence, there is a feedback loop between amyloid and neuroinflammation through activating C/EBPβ in microglia or astrocytes.

Most recently, we reported that reduction of BDNF/TrkB signaling was inversely coupled with C/EBPβ and δ-secretase escalation in AD brains (42). Furthermore, as a well-defined risk factor of AD, TBI on the cortex stimulates C/EBPβ activation and δ-secretase up-regulation, leading to AD-related pathologies and cognitive dysfunction through spreading of APP C586 and Tau N368 fragments specifically generated by active δ-secretase in 3xTg mice. In addition, chronic TBI triggers AD-like pathological events, including senile plaque and NFT in C57BL/6 mice 12 mo after injury (33). Besides, diabetes mellitus (DM) and cerebrovascular disease are age associated and common in the elderly, those most at risk for AD (43). During aging, BDNF and TrkB receptors are decreased in the brain (44). To examine the pathological roles of TBI, DM, and CCH in conjunction with reduced BDNF/TrkB in AD pathogenesis, we studied experimental models of each process in $BDNF^{+/-}$ and $TrkB^{+/-}$ mice and their wild-type (WT) littermates. Here, we show that TBI, HFD, and CCH augment AD-like pathologies in BDNF/TrkB-deficient mice compared to WT mice through activation of the C/EBPβ/δ-secretase pathway. Notably, TBI-treated $TrkB^{+/-}$ mice developed AD-associated pathologies (i.e., senile plaques and NFT) associated with neuroinflammation and extensive neuronal degeneration in association with substantial cognitive impairment. TBI-elicited senile plaques and Tau pathologies displayed spatiotemporal distributions in mice in a pattern akin to AD. Hence, TBI-treated $TrkB^{+/-}$ mice might provide a long-awaited AD-related mouse model.

Results

The C/EBPβ/δ-secretase Pathway Is Activated in $BDNF^{+/-}$ and $TrkB^{+/-}$ Mice Age Dependently. First, we assessed aging-related changes in the C/EBPβ/δ-secretase pathways in $BDNF^{+/-}$ mice, $TrkB^{+/-}$ mice, and their WT littermates in the hippocampus regions. Immunoblotting revealed that pTrkB Y816 was reduced in both $BDNF^{+/-}$ and $TrkB^{+/-}$ versus WT mice. Though pTrkB and its downstream pAKT and pMAPK were decreased in both $BDNF^{+/-}$ and $TrkB^{+/-}$ mice, associated neurotrophic signaling was abrogated more in $TrkB^{+/-}$ mice than $BDNF^{+/-}$ mice (Fig. 1*A*, top seven panels). Interestingly, C/EBPβ levels were increased in both $BDNF^{+/-}$ and $TrkB^{+/-}$ mice compared to WT mice, but the effect was greater in $BDNF^{+/-}$ mice (Fig. 1*A*, eighth and ninth panels). Accordingly, δ-secretase (AEP) was elevated in both $BDNF^{+/-}$ and $TrkB^{+/-}$ mice when C/EBPβ was increased, resulting its age-dependent escalation and activation. Consequently, the substrate Tau was robustly cleaved by δ-secretase as viewed by Tau N368 immunoblotting (Fig. 1*A*, 10th and 11th panel). qRT-PCR analysis demonstrated that *Cebpb* messenger RNA (mRNA) levels were increased in an age-dependent manner with $BDNF^{+/-}$ and $TrkB^{+/-}$ mice significantly more than WT littermates, as was downstream target *Lgmn* mRNA (Fig. 1*B*). δ-secretase activity aligned with its expression levels (Fig. 1*C*), in agreement with our previous report (34). Nonetheless, neither inflammatory cytokines nor Aβ peptides were altered with respect to age in these mice (Fig. 1 *D* and *E*). Hence, C/EBPβ/δ-secretase is up-regulated in an age-dependent manner, and depletion of BDNF/TrkB magnifies this effect.

TBI Elicits C/EBPβ/δ-Secretase Activation and AD-Like Pathologies in $BDNF^{+/-}$ and $TrkB^{+/-}$ Mice. To test whether TBI activates the C/EBPβ/δ-secretase pathway and elicits AD pathologic changes in $BDNF^{+/-}$ and $TrkB^{+/-}$ mice, we examined relevant expression levels 3 mo after TBI exposure. Compared to sham-treated control mice, C/EBPβ was increased by TBI in the hippocampus of WT mice, as were its pC/EBPβ signals, which were further increased in the hippocampus of $TrkB^{+/-}$ and $BDNF^{+/-}$ mice. δ-secretase protein levels, and the proteolytic active form, oscillated with C/EBPβ activities. Subsequently, δ-secretase-truncated Tau N368 and APP N585 fragments were prominently elevated, in alignment with δ-secretase activation (Fig. 2*A*, top eight panels). Correspondingly, Tau was hyperphosphorylated as revealed by AT8 (Fig. 2*A*, ninth panel). Immunofluorescent analysis with the brain sections showed that both Aβ and APP C586 were increased in WT mice after TBI treatment versus sham WT control and these activities were augmented in $TrkB^{+/-}$ and $BDNF^{+/-}$ mice, in alignment with our immunoblotting results; similar activities were identified with both AT8 and Tau N368 staining (Fig. 2*B*, top and second panels). As expected, δ-secretase was induced in $TrkB^{+/-}$ and $BDNF^{+/-}$ mice exposed to TBI, as was Iba1, a marker of microglial activation. MAP2-stained neurons were reduced in TBI-treated $TrkB^{+/-}$ mice and $BDNF^{+/-}$ mice as compared to WT mice, which was also validated with apoptotic active–caspase-3 staining. Compared to sham control, TBI induced neuronal loss in WT mice (Fig. 2*B*, third and fourth panels). Quantification of the fluorescent signals is summarized in Fig. 2 *B*, *Lower*. qRT-PCR analysis showed that both *Cebpb* and *Lgmn* mRNA levels were noticeably elevated in association with TBI and increased in both $BDNF^{+/-}$ and $TrkB^{+/-}$ mice versus WT mice (Fig. 2*C*). Mounting evidence points to alterations in synaptic integrity and plasticity as an early manifestation in the pathogenesis of AD and specifically to Aβ as the potential synaptotoxic factor (ref. 45 for review). Synapse density is significantly decreased in the AD brain (46), so we assessed synapses in TBI-exposed mice using electron microscopy (EM). Ultrastructural analysis demonstrated reduced synapses in TBI-exposed $TrkB^{+/-}$ and $BDNF^{+/-}$ mice compared with WT sham and TBI controls (Fig. 2*D*). Quantitative assessment

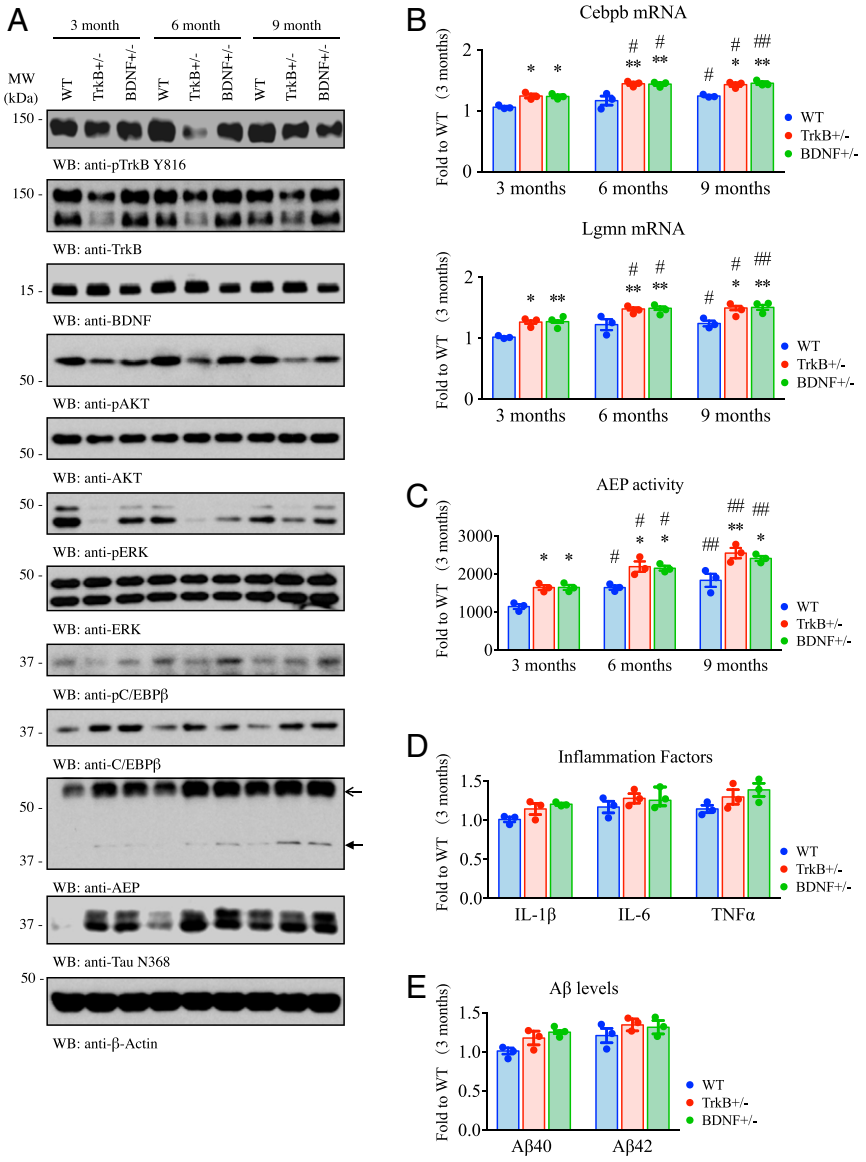

Fig. 1. Reduction of BDNF/TrkB signal initiates C/EBPβ/δ-secretase activation in an age-dependent manner. (*A*) Western blot analysis of C/EBPβ and δ-secretase activation in both TrkB$^{+/-}$ and BDNF$^{+/-}$ mice brain during aging. C/EBPβ/δ-secretase was inversely correlated with the BDNF/TrkB signaling pathway in BDNF/TrkB hemizygous mice. The bands at 56 kDa indicate full-length AEP, and the bands at 37 kDa indicate cleaved (active) AEP. (*B*) qPCR assay demonstrated the transcriptional levels of C/EBPβ (*Cebpb*) and AEP (*Lgmn*) mRNA in different ages of BDNF/TrkB hemizygous mice (mean ± SEM, $n = 3$ mice per group, two-way ANOVA, $*P < 0.05$ as compared to WT at each age, $**P < 0.01$ as compared to WT at each age; one-way ANOVA, # $P < 0.05$, ## $P < 0.01$ as compared to 3-mo-old mice in each genotype). (*C*) AEP enzymatic activity assay showed increased levels of AEP activation in an age-dependent manner in both TrkB$^{+/-}$ and BDNF$^{+/-}$ mice brain compared to WT mice (mean ± SEM, $n = 3$ mice for each group, two-way ANOVA, $*P < 0.05$ as compared to WT in each age, $**P < 0.01$ as compared to WT in each age; one-way ANOVA, # $P < 0.05$, ## $P < 0.01$ as compared to 3-mo-old mice in each genotype. AFU, arbitrary fluorescence units). (*D*) ELISA analysis of IL-1β, IL-6, and TNFα in the brain lysates from different strains of mice. Neuroinflammatory cytokines remained comparable among WT, BDNF$^{+/-}$, and TrkB$^{+/-}$ mice at 9 mo old. (Mean ± SEM, $n = 3$ mice for each group, one-way ANOVA). (*E*) ELISA analysis of Aβ in the brain lysates from different strains of mice. Aβ40 and Aβ42 peptide levels were the same among WT, BDNF$^{+/-}$, and TrkB$^{+/-}$ mice at 9 mo old. (Mean ± SEM, $n = 3$ mice for each group, one-way ANOVA).

of dendritic spines in Golgi-stained sections also found reductions in TBI-exposed TrkB$^{+/-}$ and BDNF$^{+/-}$ mice compared with WT sham and TBI controls (Fig. 2*E*). Thus, these data suggest that TBI triggers C/EBPβ/δ-secretase pathway activation and downstream AD-like pathologies in both BDNF$^{+/-}$ and TrkB$^{+/-}$ mice.

TBI Exposure Elicits Progressive Biochemical Changes and Cognitive Dysfunction in TrkB$^{+/-}$ and BDNF$^{+/-}$ Mice. To explore whether TBI exposure exacerbated Aβ metabolic and inflammatory pathways in the brain, we evaluated multiple targets in the hippocampus at 3 and 6 mo post-TBI. As before, δ-secretase activities were elevated in all of the mice after TBI treatment compared with sham and TBI WT controls; TBI-exposed δ-secretase activities in both TrkB$^{+/-}$ and BDNF$^{+/-}$ mice were higher than WT mice (*SI Appendix*, Fig. S1*A*). Remarkably, both Aβ40 and Aβ42 were progressively increased in both TrkB$^{+/-}$ and BDNF$^{+/-}$ mice, as well as WT mice, after TBI treatment (*SI Appendix*, Fig. S1*B*). Inflammatory cytokines exhibited the same kinetic changes as Aβ peptides. Consistently, TBI elicited higher inflammatory cytokines in both TrkB$^{+/-}$ and BDNF$^{+/-}$ mice than WT mice, which were more elevated compared with sham control (*SI Appendix*, Fig. S1*C*). We hypothesized that molecular changes would translate into functional deficits, which we tested using two separate behavioral tests. TBI-exposed TrkB$^{+/-}$ and BDNF$^{+/-}$ mice

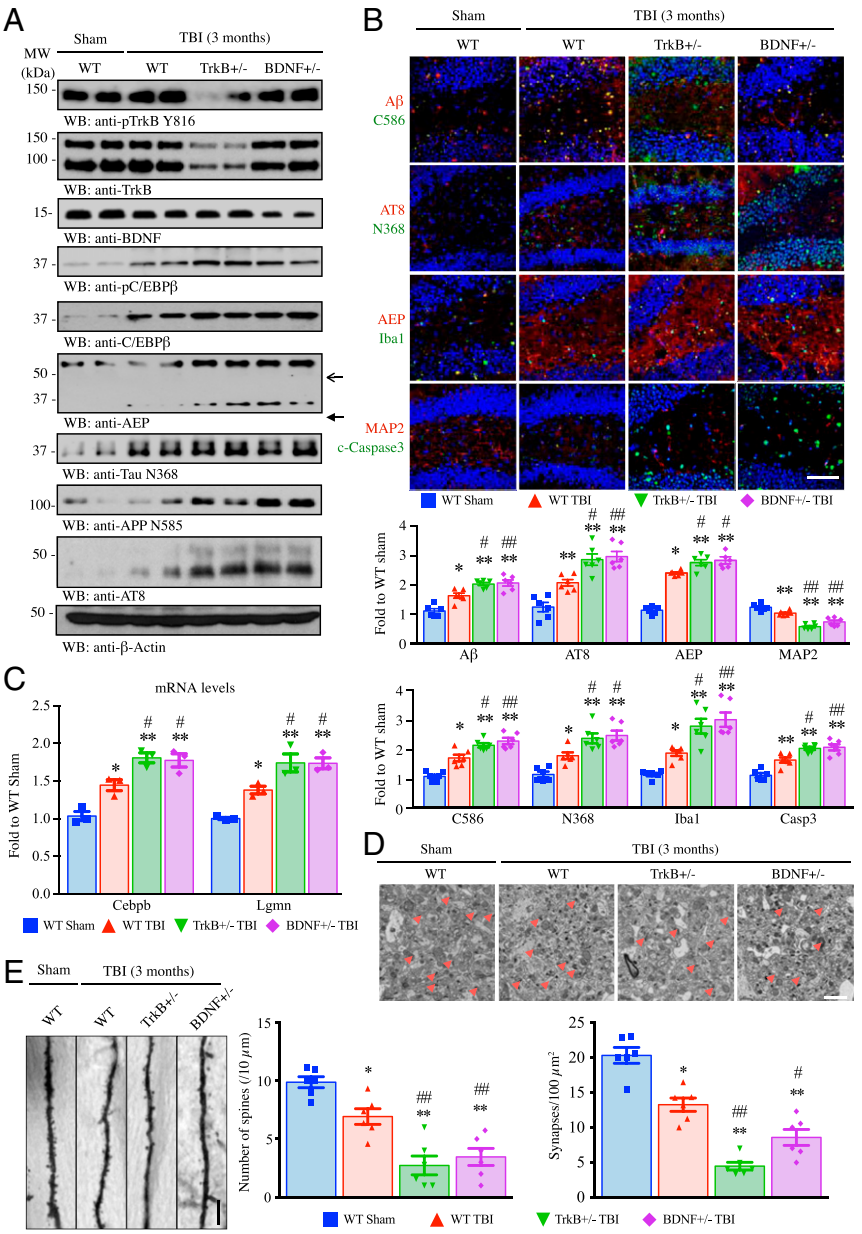

Fig. 2. TBI activates δ-secretase, mediating AD-like pathologies. (*A*) Western blot analysis of AEP activation in WT, TrkB$^{+/-}$, and BDNF$^{+/-}$ mice brain 3 mo after TBI. The bands at 56 kDa indicate full-length AEP, and the bands at 37 kDa indicate cleaved (active) AEP. (*B*) Four major AD-related pathologies are demonstrated in the frozen brain sections of WT, TrkB$^{+/-}$, and BDNF$^{+/-}$ mice 3 mo after TBI by immunofluorescence staining with antibodies of Aβ (amyloid deposition), AT8 (Tau hyperphosphorylation), Iba1 (neuroinflammation), and MAP2 (neuronal cell death) as well as cleaved-Caspase 3. The specific antibodies of AEP-cleaved APP (C586) and Tau (N368) were used for detection of AEP activation (*Upper*). Quantitative analysis the percentage of positive cells (*Lower*; mean ± SEM, $n = 6$ for each group, one-way ANOVA. $^{*}P < 0.05$, $^{**}P < 0.01$ as compared to WT sham; # $P < 0.05$ as compared to WT TBI, $^{\#\#}P < 0.01$ as compared to WT TBI). (Scale bar, 50 μm.) (*C*) qPCR assay demonstrates the transcriptional levels of C/EBPβ (*Cebpb*) and AEP mRNA (*Lgmn*). (Mean ± SEM, $n = 3$ mice per group, one-way ANOVA, $^{*}P < 0.05$, $^{**}P < 0.01$ as compared to WT sham; # $P < 0.05$ as compared to WT TBI). (*D*) EM images of the synaptic structures at CA1 region 3 mo after TBI. The arrows indicate the synapses (*Upper*). (Scale bar, 2 μm.) Quantitative analysis of the synaptic density in each group. (*Lower*; mean ± SEM, $n = 6$ mice per group, one-way ANOVA, $^{*}P < 0.05$, $^{**}P < 0.01$ as compared to WT sham; # $P < 0.05$ as compared to WT TBI, $^{\#\#}P < 0.01$ as compared to WT TBI). (*E*) Golgi staining shows the dendritic spines from the apical dendritic layer of the CA1 region (*Left*). (Scale bar, 5 μm.) Quantitative analysis of the spine density (*Right*; mean ± SEM, $n = 6$ mice for each group, one-way ANOVA. $^{*}P < 0.05$, $^{**}P < 0.01$ as compared to WT sham; # $P < 0.05$ as compared to WT TBI, $^{\#\#}P < 0.01$ as compared to WT TBI).

subjected to Morris Water Maze (MWM) showed spatial learning and memory deficits compared with TBI-exposed and sham WT controls that was not due to motor deficits affecting swimming speed (*SI Appendix*, Fig. S1*D*). Fear conditioning assay also showed more severe cognitive impairment in TBI-exposed TrkB$^{+/-}$ and BDNF$^{+/-}$ mice as compared to WT mice after TBI stimulation in both contextual fear and cued fear assays (*SI Appendix*, Fig. S1*E*). In both behavioral paradigms, impairment was more severe at 6 compared with 3 mo, consistent with injury progression over time.

Immunoblotting analysis of hippocampus tissue with 6-mo samples after TBI basically recapitulated results from 3 mo exposure latency with stronger effects in both TrkB$^{+/-}$ and BDNF$^{+/-}$ mice compared with WT mice controls (*SI Appendix*, Fig. S2*A*). Immunofluorescent staining showed that δ-secretase–truncated APP C-terminal fragment C586 was elevated in association with TBI in

both TrkB$^{+/-}$ and BDNF$^{+/-}$ mice compared to WT mice. Tau hyperphosphorylation marker AT8 activities oscillated with δ-secretase–cleaved Tau N368 signals, and similar effects occurred with respect to both δ-secretase intensities and microglial activation. Neuronal cell numbers (MAP2 signals) were inversely correlated with caspase-3–positive cells (*SI Appendix*, Fig. S2*B*). To assess whether Aβ production and Tau hyperphosphorylation elevation in both TrkB- and BDNF-deficient mice induced senile plaques and NFT formation 6 mo after TBI, we performed Thioflavin S (ThS) staining and found ThS-positive senile plaques in the injured cortex (lesion), hippocampus (HC), entorhinal cortex (EC), and around the third ventricle (V3) regions in TBI-exposed TrkB$^{+/-}$ mice. This effect was also apparent, to a lesser extent, in TBI-exposed BDNF$^{+/-}$ mice but was barely observed in WT mice exposed to TBI (*SI Appendix*, Fig. S2*C*, first and fourth columns). In alignment with these observations, AT8 and ThS double staining also revealed Tau aggregated into NFT-like structures in cortex regions of TrkB$^{+/-}$ mice, and these were also demonstrable in EC and V3 areas (*SI Appendix*, Fig. S2*C*, second and fifth columns). These effects were decreased in BDNF$^{+/-}$ mice and not identified in WT mice (*SI Appendix*, Fig. S2*C*, third and sixth columns). Both Golgi staining and EM analysis confirmed reduction in dendritic spines and synapses in TrkB$^{+/-}$ and BDNF$^{+/-}$ mice compared with WT mice 6 mo after TBI exposure (*SI Appendix*, Fig. S2 *D* and *E*). From these data, we conclude that TBI induces C/EBPβ/δ-secretase activation in TrkB- or BDNF-deficient mice, leading to progressive development of AD pathologic changes and cognitive deficits.

HFD Induces C/EBPβ/δ-Secretase Activation and AD-Like Pathologies in BDNF$^{+/-}$ and TrkB$^{+/-}$ Mice. Epidemiologic studies show that AD is associated with type 2 diabetes and obesity. Interestingly, 3xTg AD mouse model displays an age-dependent glucose tolerance impairment (47). HFD-induced obesity is a broadly utilized type 2 diabetes model. To assess the crosstalk between diabetes and neurotrophic activities reduction in AD pathologies, we employed 2-mo-old TrkB$^{+/-}$ and BDNF$^{+/-}$ mice and WT littermate and fed them with HFD or chow diet control for 3 mo. As expected, both TrkB and BDNF heterozygous mice gained weight faster than WT littermate by HFD, which grew faster than WT mice under chow diet. After 3 mo, both TrkB$^{+/-}$ and BDNF$^{+/-}$ mice were more obese than WT mice upon HFD. Both male and female mice exhibited similar growth curves (*SI Appendix*, Fig. S3 *A* and *B*). Interestingly, pTrkB signals in the hippocampus area were not affected by HFD in WT and BDNF$^{+/-}$ mice as compared to chow diet in WT mice. Depletion of TrkB evidently reduced its p-816 activities. Blatantly, C/EBPβ levels were increased by HFD in TrkB$^{+/-}$ and BDNF$^{+/-}$ mice versus the WT littermate. In contrast, C/EBPβ was barely detectable under chow control in WT mice. HFD also incurred strong pC/EBPβ activation versus chow diet in WT mice (Fig. 3*A*, top to fifth panels). Accordingly, δ-secretase was augmented, closely coupled to C/EBPβ levels. Correspondingly, APP N585 and Tau N368 were truncated by active δ-secretase, and Tau phosphorylation AT8 activities fitted well with Tau N368 levels (Figs. 3*A*, sixth to ninth panel). Immunofluorescent analysis showed that HFD elicited more APP C586 truncation than chow diet, and Aβ staining in the hippocampus was more prominent in TrkB$^{+/-}$ and BDNF$^{+/-}$ mice than WT mice (Fig. 3 *B*, *Top*). AT8 and Tau N368 costaining also exhibited a similar pattern (Fig. 3*B*, second panel). Noticeably, microglia activation indicated by Iba1 staining was escalated upon HFD as compared to chow diet. MAP2 and active caspase-3 costaining showed that neurons were reduced upon HFD treatment, and neuronal apoptotic activities were increased in both TrkB$^{+/-}$ and BDNF$^{+/-}$ mice (Fig. 3*B*, third and fourth panels). Quantification of immunofluorescent signals verified these observations (Fig. 3 *B*, *Lower*). δ-secretase enzymatic activities displayed the similar pattern as revealed by immunoblotting (Fig. 3*C*). Again, qRT-PCR also supported HFD prominently elevated both *Cebpb* and *Lgmn* mRNAs, fitting with their proteins' abundance by immunoblotting (*SI Appendix*, Fig. S3*B*). HFD also provoked more inflammatory cytokines production than chow diet with TrkB$^{+/-}$ and BDNF$^{+/-}$ mice stronger than WT mice (*SI Appendix*, Fig. S3*C*). The enzyme-linked immunosorbent assay (ELISA) revealed a similar effect with Aβ40 and Aβ42 levels (Fig. 3*D*). EM analysis of synapses indicated that HFD incurred extensive synaptic loss in TrkB$^{+/-}$ and BDNF$^{+/-}$ mice, which exhibited more prominent effects than WT mice (*SI Appendix*, Fig. S3*D*). We made similar observations with dendritic spines by Golgi staining (*SI Appendix*, Fig. S3*E*). MWM assay showed that HFD triggered the poorest cognitive deficits with TrkB$^{+/-}$, followed by BDNF$^{+/-}$ mice and then WT mice as compared to chow diet–treated WT mice (Fig. 3*E*). However, these mice displayed similar swimming speed, suggesting that the motor functions are comparable among the mice (*SI Appendix*, Fig. S3*F*). Fear conditioning assay validated the cognitive performance results in MWM, with TrkB$^{+/-}$ mice revealing the worst cognitive impairments (Fig. 3*F*). Together, these data support that HFD elicits robust C/EBPβ/δ-secretase pathway activation, resulting in pronounced Aβ production and Tau hyperphosphorylation in TrkB$^{+/-}$ and BDNF$^{+/-}$ mice. The dramatic synaptic loss, associated with potent neuroinflammation, incurs notable cognitive defects.

CCH Triggers C/EBPβ/δ-Secretase Activation and AD-Like Pathologies in BDNF$^{+/-}$ and TrkB$^{+/-}$ Mice. To explore whether CCH triggers AD-like pathologies in BDNF/TrkB-deficient mice, we conducted the bilateral partial carotid artery occlusion and monitored the brain blood flow using Doppler radar. We found that the blood velocity under the common carotid artery (CCA) and the internal carotid artery (ICA) were reduced 3 mo after ligation compared to Pretest. The diameter under CCA was reduced versus Pretest (*SI Appendix*, Fig. S4*A*). Under CCH stress, pTrkB activities in WT and BDNF$^{+/-}$ mice remained comparable to sham control. However, both C/EBPβ and pC/EBPβ were increased as compared to sham control in WT mice, with the most profound elevation in TrkB$^{+/-}$ mice, followed by BDNF$^{+/-}$ and WT mice. Accordingly, δ-secretase was augmented and activated by echoing C/EBPβ activation, which led to both Tau N368 and APP N585 cleavage by active δ-secretase. Consequently, AT8 was enhanced, correlating with Tau proteolytic cleavage activities (Fig. 4*A*). Immunofluorescent costaining revealed that CCH robustly elicited both Aβ and AT8 activities in the hippocampus with TrkB$^{+/-}$ mice the strongest, whereas these signals were barely detectable under sham control. The truncated APP C586 and Tau N368 were also demonstrable under CCH in TrkB$^{+/-}$ mice (Fig. 4*B*, top and second panels). CCH treatment incurred Iba1 signal augmentation compared to sham control, associated with evident δ-secretase up-regulation, with the most robust activity in TrkB$^{+/-}$ mice, followed by BDNF$^{+/-}$ mice (Fig. 4*B*, third panel). In consequence, extensive neuronal apoptosis was initiated by CCH, with the most robust effect in TrkB$^{+/-}$ mice, as revealed by MAP2/active caspase-3 costaining (Fig. 4 *B*, *Bottom*). Quantification of the immunofluorescent signal intensities is summarized in the *Lower* panels of Fig. 4*B*. The enzymatic assay showed that δ-secretase was highly activated under CCH, which also elicited both Aβ40 and 42-peptide up-regulation (Fig. 4 *C* and *D*). qRT-PCR analysis showed that CCH significantly augmented *Cebpb* and *Lgmn* mRNA levels, with the most abundant in TrkB/BDNF-deficient mice, fitting with their protein levels increase (*SI Appendix*, Fig. S4*B*). In alignment with the pronounced microglia cell activation, inflammatory cytokines (i.e., IL-1β, IL-6, and TNFα) were all enhanced under CCH stress versus sham control (*SI Appendix*, Fig. S4*C*). Quantitative synapse analysis with EM showed that CCH triggered extensive synaptic loss in both TrkB$^{+/-}$ and BDNF$^{+/-}$ mice as compared to WT or the sham control (*SI Appendix*, Fig. S4*D*). Golgi staining indicated the similar reduction pattern with the dendritic spines (*SI Appendix*, Fig. S4*E*). Noticeably, MWM test demonstrated that CCH provoked cognitive dysfunction versus sham control, and TrkB$^{+/-}$ and BDNF$^{+/-}$ mice spent less time in the target quadrant compared to WT mice, fitting with the

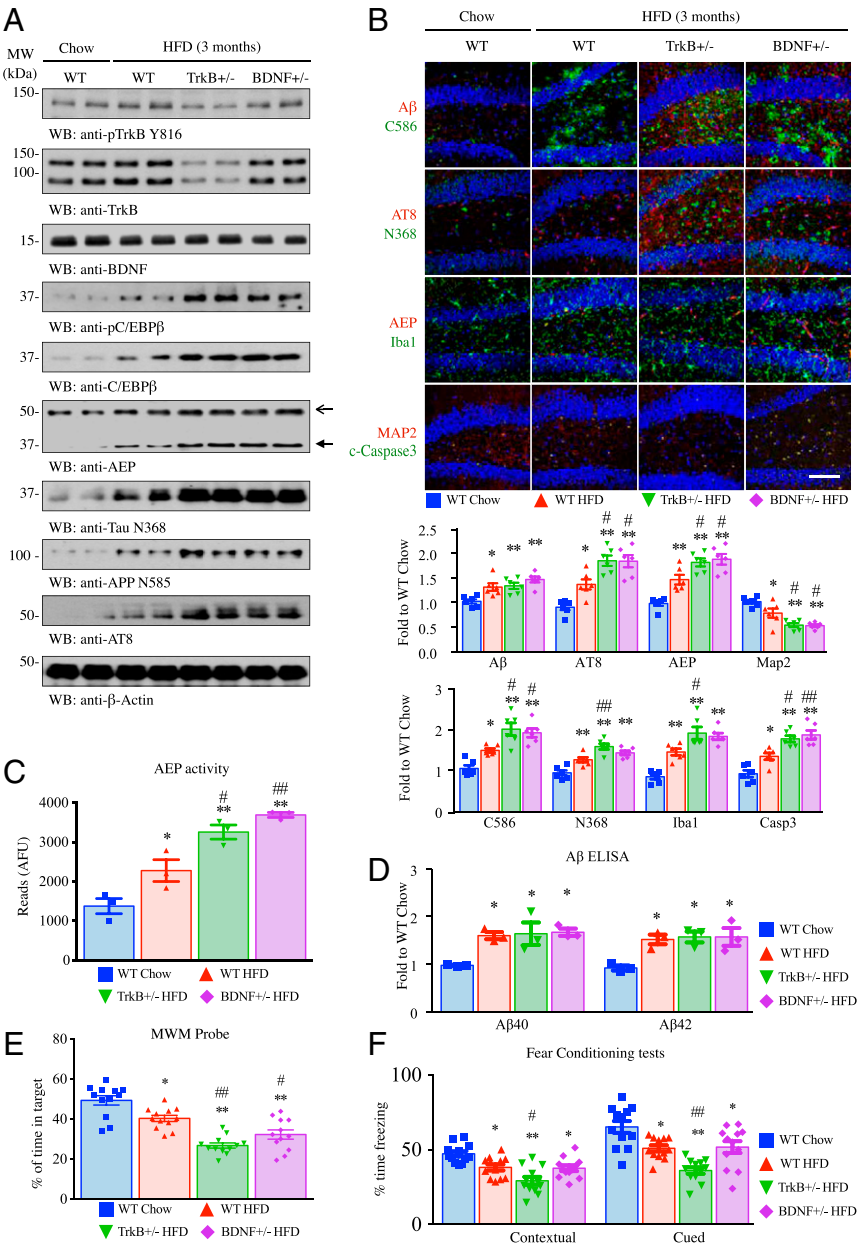

Fig. 3. HFD activates AEP, mediating AD-like pathologies. (*A*) Western blot analysis of AEP activation in WT, TrkB$^{+/-}$, and BDNF$^{+/-}$ mice feeding with HFD for 3 mo. The bands at 56 kDa indicate full-length AEP, and the bands at 37 kDa indicate cleaved (active) AEP. (*B*) AD-related pathologies were demonstrated in WT, TrkB$^{+/-}$, and BDNF$^{+/-}$ mice at 3 mo after HFD by immunofluorescence with antibodies of Aβ, AT8, Iba1, and MAP2 as well as cleaved-Caspase3 staining. The specific antibodies of AEP, APP C586, and Tau N368 were used for detection of AEP activation (*Upper*). Quantitative analysis the percentage of positive cells (*Lower*; mean ± SEM, $n = 6$ for each group, one-way ANOVA, $*P < 0.05$, $**P < 0.01$ as compared to WT chow; # $P < 0.05$ as compared to WT HFD). (Scale bar, 50 μm.) (*C*) AEP enzymatic activity assay showed the AEP activation was increased in both TrkB$^{+/-}$ and BDNF$^{+/-}$ mice brain after HFD, compared to WT mice (mean ± SEM, $n = 3$ mice for each group, one-way ANOVA, $*P < 0.05$, $**P < 0.01$ as compared to WT chow; # $P < 0.05$ as compared to WT HFD; AFU, arbitrary fluorescence units). (*D*) ELISA quantification of Aβ40 and Aβ42 in WT, TrkB$^{+/-}$, and BDNF$^{+/-}$ mice brain 3 mo after HFD. HFD increased Aβ levels regardless of genotypes (mean ± SEM, $n = 3$ mice for each group, one-way ANOVA, $*P < 0.05$ as compared to WT chow, no significant difference was observed among all genotypes of mice fed with HFD). (*E*) MWM analysis as the percentage of time spent in the target quadrant in the probe trial. (Mean ± SEM, $n = 12$ mice for each group, one-way ANOVA, $*P < 0.05$, $**P < 0.01$ as compared to WT chow; # $P < 0.05$, ## $P < 0.01$ as compared to WT HFD.) (*F*) Contextual and cued fear conditioning was reduced in TrkB$^{+/-}$ and BDNF$^{+/-}$ mice after HFD, compared with WT group (mean ± SEM, $n = 12$ mice per group, one-way ANOVA, $*P < 0.05$, $**P < 0.01$ as compared to WT chow; # $P < 0.05$ as compared to WT HFD).

pronounced synaptic loss in these mice (Fig. 4*E*). Fear conditioning tests revealed similar results (Fig. 4*F*). Hence, CCH strongly induces C/EBPβ and δ-secretase expression in BDNF/TrkB-deficient mice, leading to AD-like pathologies and cognitive dysfunctions.

TBI Provokes Senile Plaques and NFT Tempospatial Distribution in TrkB$^{+/-}$ Mice. In AD, Aβ deposition precedes neurofibrillary and neuritic changes with an apparent origin in the frontal and temporal lobes, hippocampus, and limbic system. The neurofibrillary tangles and neuritic degeneration start in the medial temporal lobes and hippocampus and progressively spread to other areas of the neocortex (48). Among these three environmental risk factors, the most pronounced AD-like pathologies occurred in TrkB$^{+/-}$ mice. To further investigate those pathologies in spatial distribution in TrkB$^{+/-}$ mice, we compared the effects induced by TBI, HFD, and CCH on δ-secretase activation and subsequent

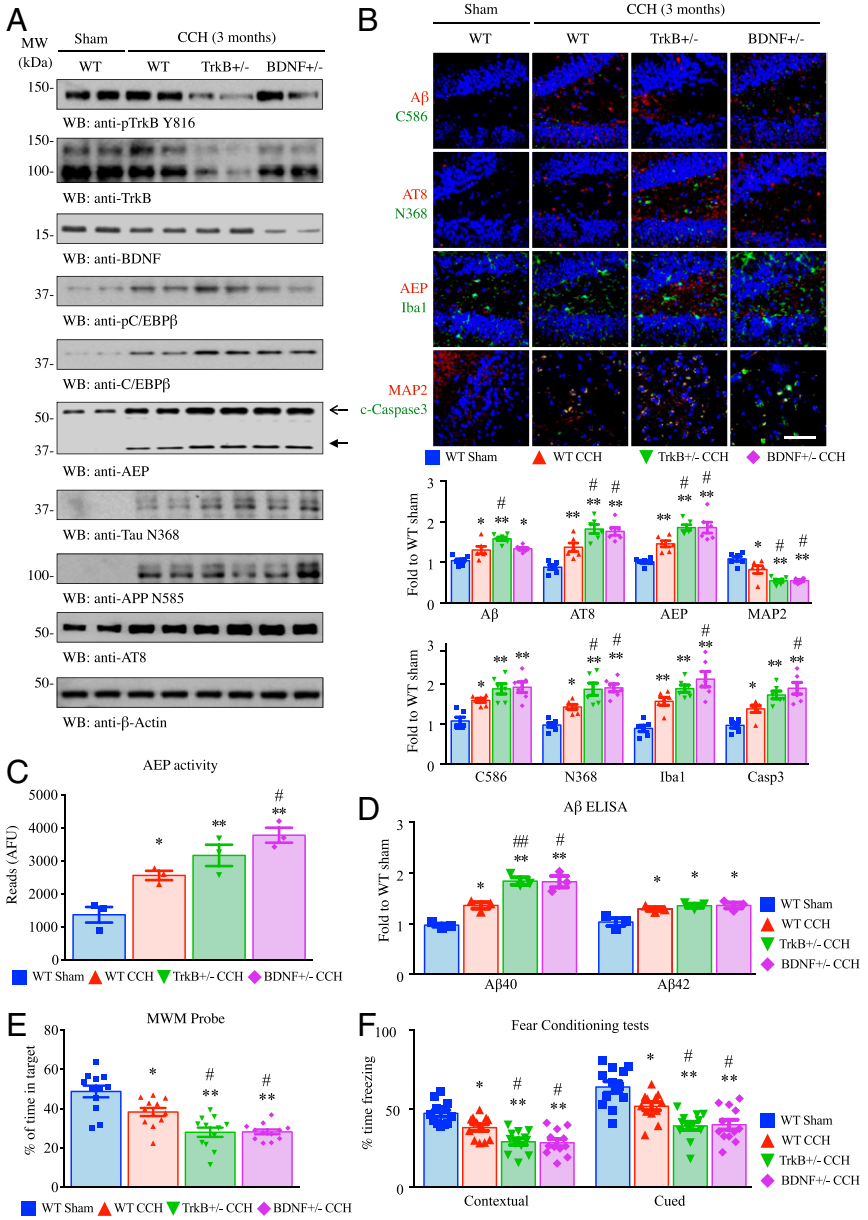

Fig. 4. CCH activates AEP, mediating AD-like pathologies. (*A*) Western blot analysis of AEP activation in WT, TrkB$^{+/-}$, and BDNF$^{+/-}$ mice with CCH for 3 mo. The bands at 56 kDa indicate full-length AEP, and the bands at 37 kDa indicate cleaved (active) AEP. (*B*) AD-related pathologies were demonstrated in WT, TrkB$^{+/-}$, and BDNF$^{+/-}$ mice at 3 mo after CCH by immunofluorescence with antibodies of Aβ, AT8, Iba1, and Map2 as well as cleaved-Caspase3 staining. The specific antibodies of AEP, APP C586, and Tau N368 were used for detection of AEP activation (*Upper*). Quantitative analysis of the percentage of positive cells (*Lower*; mean ± SEM, $n = 6$ for each group, one-way ANOVA, $^{*}P < 0.05$, $^{**}P < 0.01$ as compared to WT sham; # $P < 0.05$ as compared to WT CCH, $^{\#\#}P < 0.01$ as compared to WT CCH). (Scale bar, 50 μm.) (*C*) AEP enzymatic activity assay showed AEP activation is increased in both TrkB$^{+/-}$ and BDNF$^{+/-}$ mice brain after CCH compared to WT mice (mean ± SEM, $n = 3$ mice for each group, one-way ANOVA, $^{*}P < 0.05$ as compared to WT sham; # $P < 0.05$ as compared to WT CCH; AFU, arbitrary fluorescence units). (*D*) ELISA quantification of Aβ40 and Aβ42 in WT, TrkB$^{+/-}$, and BDNF$^{+/-}$ mice brain 3 mo after CCH (mean ± SEM, $n = 3$ mice for each group, one-way ANOVA, $^{*}P < 0.05$, $^{**}P <$ 0.01 as compared to WT sham; # $P < 0.05$ as compared to WT CCH, $^{\#\#}P < 0.01$ as compared to WT CCH). (*E*) MWM analysis as the percentage of time spent in the target quadrant in the probe trial was recorded and analyzed (mean ± SEM, $n = 12$ mice for each group, one-way ANOVA, $^{*}P < 0.05$, $^{**}P < 0.01$ as compared to WT sham; # $P < 0.05$ as compared to WT CCH). (*F*) Contextual fear conditioning was impaired in TrkB$^{+/-}$ and BDNF$^{+/-}$ mice after CCH compared with WT group (mean ± SEM, $n = 12$ mice for each group, one-way ANOVA, $^{*}P < 0.05$ as compared to WT sham; # $P < 0.05$ as compared to WT CCH).

biochemical events in different brain regions. Immunoblotting revealed that TBI elicited the most abundant δ-secretase. Accordingly, APP N585 and Tau N368 fragmentation and Tau phosphorylation (AT8) activities fluctuated with δ-secretase activation. TBI-induced effects were the strongest among the three risk factors (Fig. 5*A*). Silver staining indicated that these three risk factors triggered more plentiful positive inclusions in the cortex than sham control. Markedly, CCH elicited the aggregates mainly resided intraneuronally, whereas TBI and HFD incurred both extracellular and intraneuronal deposits. The similar effect was observed in the hippocampus with TBI the strongest among the three risk factors (Fig. 5*B*). The enzymatic assay demonstrated that δ-secretase was activated by TBI in more regions than HFD and CCH, in alignment with its active fragment abundance (Fig. 5*C*). To further assess the characteristic features of the aggregates, we conducted Aβ/THS or AT8/ThS costaining with the

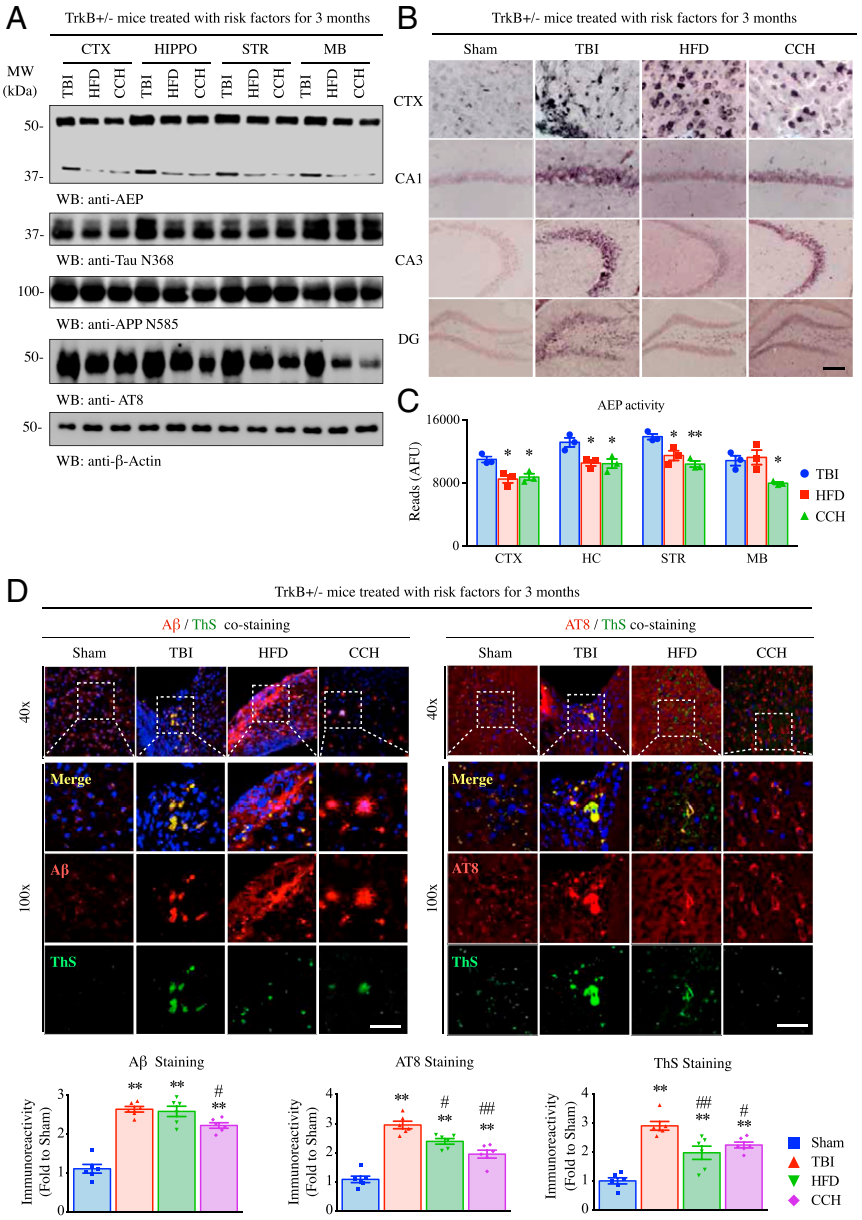

Fig. 5. The spatial comparison of amyloid deposition and Tauopathy among TBI, HFD, and CCH in TrkB $^{+/-}$ mice. (*A*) Western blot analysis of AEP activation, Tau/APP cleavages, and Tau hyperphosphorylation in TBI, HFD, and CCH models. (*B*) Gallyas silver staining for senile plaque and NFT at cortex (CTX) and hippocampus CA1, CA3, and DG regions in the TrkB$^{+/-}$ mice brain 3 mo after TBI, HFD, or CCH treatment. (Scale bar, 50 μm.) (*C*) AEP enzymatic activity assay showed AEP activation at cortex (CTX), hippocampus (HC), striatum (STR), and middle brain (MB) among the models of TBI, HFD, and CCH in TrkB $^{+/-}$ mice (mean ± SEM, $n = 3$ mice for each group, one-way ANOVA, $^{*}P < 0.05$, $^{**}P < 0.01$ as compared to TrkB$^{+/-}$ TBI cortex; AFU, arbitrary fluorescence units). (*D*) The formation of amyloid plaques and NFT in TrkB$^{+/-}$ mice after TBI, HFD, and CCH were shown by costaining of Thioflavin-S (ThS) + Aβ and ThS + AT8, respectively (*Upper*). (Scale bar, 30 μm.) Quantitative analysis of plaque size and the intensity of Aβ, AT8, and ThS (*Lower*; mean ± SEM, $n = 6$ mice in each group, one-way ANOVA, $^{*}P < 0.05$, $^{**}P < 0.01$ as compared to TrkB$^{+/-}$ sham; # $P < 0.05$ as compared to TrkB$^{+/-}$ TBI, $^{\#\#}$ $P < 0.01$ as compared to TrkB$_{+/-}$ TBI).

brain sections. Compared to sham control, these three risk factors provoked demonstrable senile plaques in the cortex that were both Aβ and ThS positive, and the similar effects occurred to AT8/ThS costaining as well. It is worth noting that the effects by TBI were the most prominent among the three risk factors (Fig. 5 *D*, *Upper*). The quantification is summarized in Fig. 5 *D*, *Lower*. Both Aβ and AT8 activities were stained by immunohistochemistry (IHC) in different brain areas from TrkB$^{+/-}$ mice 3 mo after TBI, HFD, and CCH treatment (*SI Appendix*, Fig. S5*A*). Clearly, TBI provoked more extensive Aβ deposit in the lesioned cortex, followed by hippocampus and brainstem. Noticeably, HFD also initiated more massive Aβ signals in the cortex and hippocampus than CCH. TBI incited widespread AT8 activities enriched in the cortex, fiber tracts, and brainstem, whereas HFD- and CCH-aggravated AT8 signals mainly resided in the fiber tracts and brainstem. The collective Aβ and AT signals by these stresses were shown in the schematic map (*SI Appendix*, Fig. S5*B*). To test whether Aβ and Tau aggregates in the mice 3 mo after TBI, HFD, or CCH stimulation could spread into other neurons, we prepared primary cortical neurons from TrkB$^{+/-}$ neonatal pups and incubated the cells with brain lysates from different mice treated with the three risk factors for 17 h. Immunofluorescent costaining with antibodies against Aβ and APP C586 revealed that TBI-treated TrkB$^{+/-}$ or BDNF$^{+/-}$ mice brain lysates elicited the strongest Aβ

signals in primary cortical neurons, followed by HFD and CCD, compared to the basal noises from the control intact brain lysates. WT mice revealed the weakest activities. δ-secretase–truncated APP C586 signals were aggregated and mainly associated with neurite processes (*SI Appendix*, Fig. S5 *C*, *Left*). We made similar observations with AT8/Tau N368 costaining activities (*SI Appendix*, Fig. S5 *C*, *Right*). Together, the studies suggest that TBI elicits the conspicuous Aβ deposition and NFT pathologies in the brain areas in $TrkB^{+/-}$ mice, which are vulnerable in AD patient brains with accumulation of both pathological features.

Depletion of C/EBPβ Blocks TBI-Induced AD Pathologies. The above studies demonstrated that C/EBPβ mediates δ-secretase expression in response to the risk factor stimulation, triggering the downstream pathological events. To determine the pathological roles of C/EBPβ in TBI-induced AD-like pathologies, we injected lentivirus overexpressing a small hairpin RNA (shRNA) of C/EBPβ with the green fluorescent protein (GFP) termed as C/EBPβ-shRNA-GFP or control-GFP virus into the hippocampus of different mice 1 wk before TBI treatment. We monitored its expression by immunoblotting 3 mo after TBI treatment and found that TBI-elicited C/EBPβ was evidently reduced by its specific shRNA as compared to the control virus. δ-secretase levels coupled with its upstream transcription factor C/EBPβ. Consequently, the proteolytic truncates of APP N585 and Tau N368 closely mirrored δ-secretase concentrations, so were hyperphosphorylated AT8 activities (*SI Appendix*, Fig. S6*A*). Knockdown of C/EBPβ repressed TBI-induced Aβ production (*SI Appendix*, Fig. S6*B*). δ-secretase enzymatic assay demonstrated that depletion of C/EBPβ diminished its protease activities (*SI Appendix*, Fig. S6*C*). Furthermore, TBI-incurred inflammatory cytokines were potently attenuated when C/EBPβ was depleted, fitting with its transcriptional roles for these cytokines (*SI Appendix*, Fig. S6*D*). To further validate these findings, we conducted an immunofluorescent costaining study and found that TBI-induced Aβ production and Tau hyperphosphorylation (AT8) were significantly reduced when C/EBPβ was knocked down, so were truncated APP C586 and Tau N368 levels and their upstream protease δ-secretase (*SI Appendix*, Fig. S7 *A*, *Left*). Quantitative analysis of Iba1 levels in active microglia also fitted with inflammatory cytokines. Depletion of C/EBPβ substantially increased neuronal survival as reviewed by MAP2 signals, inversely coupled with the reduction of active caspase-3 (*SI Appendix*, Fig. S7 *A*, *Right*). Both Golgi staining and EM analysis demonstrated that the dendritic spines and the synapses in TBI-struck brains were elevated upon C/EBPβ depletion (*SI Appendix*, Fig. S7 *B* and *C*). Accordingly, MWM cognitive behavioral test showed that TBI-elicited memory deficits were alleviated when C/EBPβ was deleted (*SI Appendix*, Fig. S6*E*). The similar discoveries were found in both contextual fear and cued fear behavioral assays (*SI Appendix*, Fig. S6*F*). Therefore, these studies strongly support that TBI-induced C/EBPβ plays a critical role in mediating δ-secretase up-regulation and subsequent AD pathologies in BDNF/TrkB-deficient mice.

BDNF/TrkB Reduction and C/EBPβ/δ-Secretase Pathway Activation in Human TBI Patients. To validate the findings in animal models, we performed immunoblotting with TBI and AD patient brains, pTrkB activation was reduced the most in AD, followed by TBI patients as compared to healthy control, and BDNF levels correlated with TrkB activation patterns (Fig. 6*A*, top three panels). Both pC/EBPβ and its total levels inversely coupled with BDNF/pTrkB signals, and its downstream target δ-secretase closely correlated with the transcription factor activities (Fig. 6*A*, fourth and fifth panels). Accordingly, both APP N585 and Tau N368 truncates and AT8 fitted with their upstream protease (Fig. 6*A*, sixth to ninth panels). Immunofluorescent staining revealed the reduction of both BDNF and pTrkB in AD and TBI brains, which were conversely correlated with C/EBPβ and δ-secretase levels (Fig. 6*B*). Therefore, TBI elicits BDNF/TrkB signaling pathway reduction, which results in up-regulation of C/EBPβ/δ-secretase and enhances proteolytic APP and Tau fragmentation, reflecting the events occur in human AD patients.

Discussion

In the current report, we show that C/EBPβ and its downstream target δ-secretase are elevated and activated in $BDNF^{+/-}$ or $TrkB^{+/-}$ mice in an age-dependent manner. Interestingly, these events are robustly augmented under stresses of TBI, HFD, or CCH. Accordingly, activated δ-secretase cleaves both APP and Tau and consequently increases Aβ and Tau phosphorylation (AT8), resulting in synaptic loss and cognitive impairments. Of note, 3 mo after TBI, there are demonstrable Aβ/ThS and AT8/ThS double-positive plaques in the hippocampus of $TrkB^{+/-}$ mice. Knockdown of C/EBPβ greatly abrogates these AD-like pathologies in $TrkB^{+/-}$ mice upon TBI stimulation, supporting that the TBI-activated C/EBPβ/δ-secretase pathway plays an essential role in mediating TBI-triggered AD-like pathologies in TrkB-deficient mice. In typical cases of AD, Aβ deposition precedes neurofibrillary and neuritic changes with an apparent origin in the frontal and temporal lobes, hippocampus, and limbic system (48). Our temporal studies show that Aβ, neuroinflammation, and cognitive defects are progressively increased in $TBI^{+/-}$ mice from 3 to 6 mo (*SI Appendix*, Fig. S1). Both Aβ and Tau pathologies spread in $TrkB^{+/-}$ mice in a tempospatial distribution pattern similar to what is observed in Braak stages as the disease progresses (*SI Appendix*, Fig. S5 *A* and *B*). Therefore, our findings indicate that TBI-treated $TrkB^{+/-}$ mice exhibit AD-like pathologies and their temporal spreading similar to what occurred in human AD patients. Currently, there is no proper animal model for sporadic AD, but an overwhelming emphasis is focused on transgenic AD models to understand the disease pathogenesis. It is intuitively illogical to assume that the pathogenesis of sporadic AD that occurs without any definite mutation would be explained by a transgenic model harboring single or multiple mutations (49). Therefore, our data demonstrate that TBI-treated $TrkB^{+/-}$ mice may provide a disease model that would simulate AD-related pathogenesis.

The molecular nature of gene–environment interaction or its temporal relationship with the pathogenesis of sporadic AD is largely unknown. The experimental research in AD for exploring disease pathogenesis has been dominated by the attempts for identification of various neurotoxic consequences of abnormal protein accumulation on one hand and on the other by extensive use of transgenic AD models harboring single- or multiple-mutant gene(s) of human familial AD (50, 51). However, this approach so far has neither explained the complexity and heterogeneity of sporadic human AD nor produced any reasonably efficacious drug for this condition. Despite a plethora of evidence from animal models (transgenic and chemical induced), cell-based models, and postmortem brain of AD subjects supporting the "Amyloid Cascade Hypothesis" or "tauopathy," it is not clear how these alterations of abnormal protein accumulation and aggregation are triggered in the aging brain, especially in the case of sporadic AD (49).

C/EBPs have been implicated in the control of biological processes critical for neuronal development and survival (52) and responses to brain injury and ischemia (53). Noticeably, $C/EBP\beta^{-/-}$ mice are more resistant to excitotoxicity-induced neuronal cell death than WT mice (54), indicating that it might regulate gene expression involved in brain injury. C/EBPs also implicate in learning and memory (55). Notably, C/EBPs are up-regulated in AD (56, 57). Aβ mediates C/EBPβ and C/EBPδ activation in glial cells (54). Most recently, we demonstrate that C/EBPβ but not C/EBPα is sufficient and necessary for δ-secretase transcription during aging and in AD pathogenesis. Depletion of C/EBPβ from aged 3xTg or 5XFAD mice abolishes AD pathologies and cognitive dysfunctions via diminishing δ-secretase expression, whereas overexpression of C/EBPβ in young 3xTg mice accelerates AD pathologies and

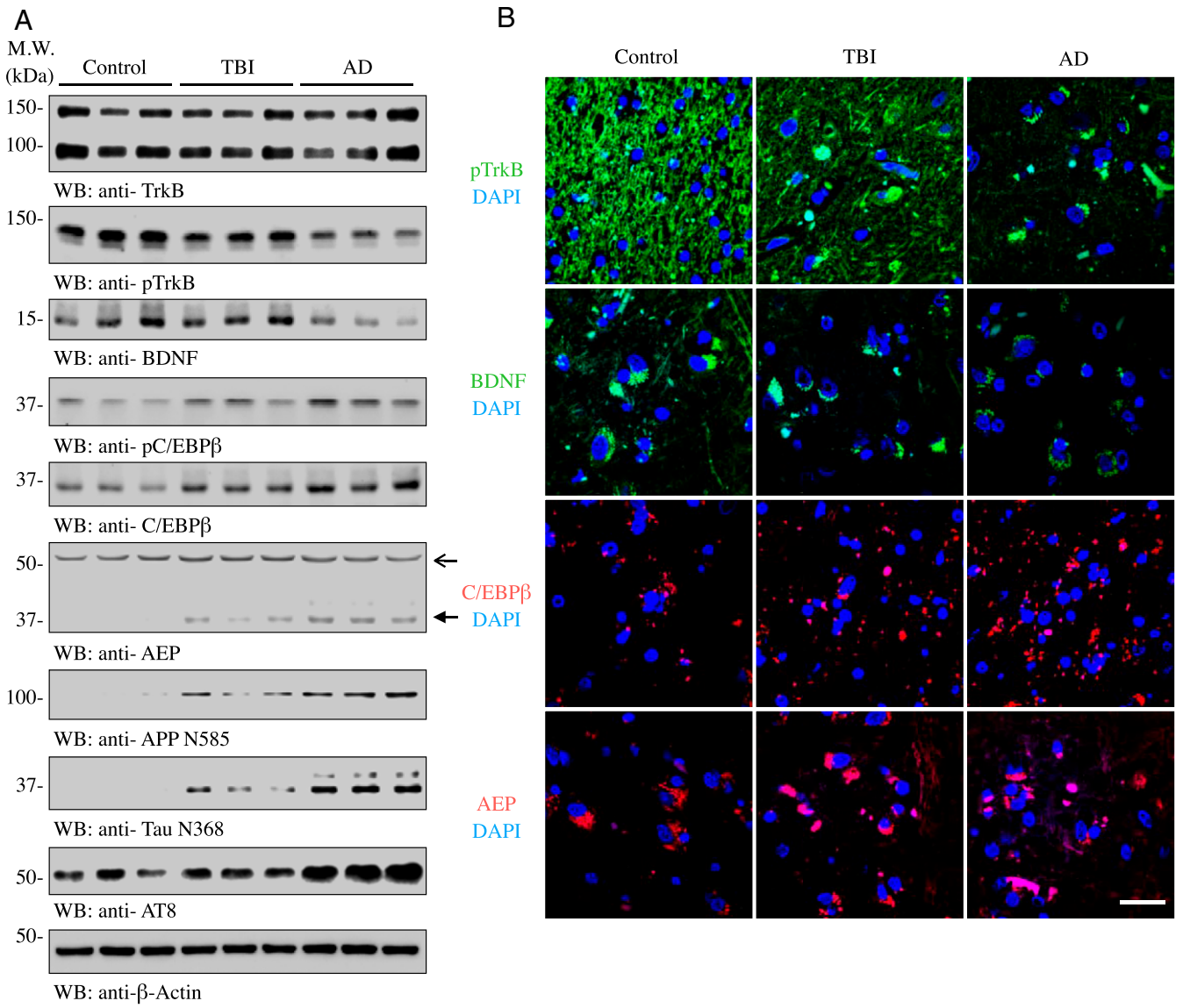

Fig. 6. BDNF/TrkB pathway reduction and C/EBPβ/δ-secretase signaling escalation in human TBI and AD brains. (*A*) Immunoblotting analysis of human control, TBI, and AD patient brain samples. BDNF and pTrkB were reduced, whereas C/EBPβ and pC/EBPβ and δ-secretase levels were augmented in both AD and TBI patients brains as compared to control. The brain lysates were analyzed by immunoblotting using indicated antibodies. The bands at 56 kDa indicate full-length AEP, and the bands at 37 kDa indicate cleaved (active) AEP. (*B*) Immunofluorescent staining of human brain sections. Both pTrkB (*Top*) and BDNF (second panels) were reduced in TBI and AD brains, whereas C/EBPβ (third panel) and AEP (*Bottom*) were escalated in both TBI and AD brains. (Scale bar, 10 μm.)

cognitive deficits via augmenting δ-secretase (34). In addition to promoting the production of inflammatory mediators, C/EBP family members and the classical proinflammatory triad of IL-1, IL-6, and TNFα mutually regulated each other (35–38). Hence, there is a vicious cycle between amyloid and neuroinflammation through activating C/EBPβ in microglia or astrocytes. Noticeably, we found that Aβ elicits δ-secretases' mRNA transcription in a C/EBPβ-dependent manner (34). Conceivably, TBI-elicited inflammation may augment C/EBPβ expression, which subsequently elevates δ-secretase levels that concurrently cleave both APP and Tau, promoting Aβ production and Tau hyperphosphorylation. These events ultimately culminate in senile plaque deposition and NFT formation. All of the discussed effects may be exacerbated in the absence of neurotrophic factors BDNF/TrkB. Accordingly, TBI-treated $TrkB^{+/-}$ mice exhibit the spatiotemporal propagation of both senile plaques and tauopathies in the brain, displaying the prominent synaptic degeneration and cognitive dysfunctions. It is worth noting that TBI did not incur the exact same AD-like pathologies in $BDNF^{+/-}$ mice as in $TrkB^{+/-}$ mice (*SI Appendix*, Fig. S2). It is understandable that deletion of a ligand is not equivalent to depletion of its receptors because TrkB receptors have both BDNF and NT-4 ligands; thus, deletion of the TrkB receptors will elicit more severe effects than one of the multiple ligands.

Several immediate early (IE) genes act as targets for BDNF/TrkB signaling for neuronal functions, and C/EBPβ is recruited to the target promoter upon BDNF treatment. BDNF induction of genes important for neuronal functions depends on up-regulation of transcription factors including C/EBPβ during neuronal development (58). Furthermore, hippocampal BDNF-positive autoregulatory feedback loop via C/EBPβ is necessary for memory consolidation. On the other hand, C/EBPβ controls an increase in expression of *bdnf* exon IV transcripts and BDNF protein, mediating

memory consolidation (59). Together, C/EBPβ plays a critical role in mediating BDNF's functions, and they mutually regulate each other in the central nervous system (CNS). Surprisingly, we found that depletion of either BDNF or TrkB increases C/EBPβ expression, resulting in δ-secretase up-regulation and inflammation escalation (Figs. 1 and 2). Although acute BDNF stimulation and chronic BDNF/TrkB signaling pathway repression provoke C/EBPβ activation, the biological consequences are completely opposite. The acute BDNF agitation mediates the neuronal development and synaptogenesis via activating C/EBPβ, whereas partial knockdown of BDNF/TrkB in their hemizygous mice elicits cognitive impairments by activating C/EBPβ-regulated malicious targets including δ-secretase, inflammatory cytokines, etc. (Figs. 1–4).

BDNF serves widespread roles in regulating energy homeostasis (60). In both humans and mice, BDNF/TrkB ablation or mutation causes hyperphagia and obesity phenotype (61–63). Interestingly, administration of BDNF into the diabetic (db/db) mice transiently increases energy metabolism (64). As expected, HFD strongly increased both $BDNF^{+/-}$ and $TrkB^{+/-}$ mice body weight more than their littermates. Subsequently, C/EBPβ/δ-secretase was highly up-regulated, leading to increased AD-like pathologies including Aβ production and AT8 that are further elevated in BDNF/TrkB-deficient mice, associated with evident synaptic loss and cognitive deficits (Fig. 3). These findings are consistent with previous reports that the levels of Aβ and proinflammatory cytokines accumulate during the brain aging and progression of AD, leading to TrkB signaling repression by Aβ, TNFα, and IL-1β, which also regulate the docking protein (e.g., IRS and Shc), suppressing insulin signaling (65). In transgenic Tg2576 AD mice, HFD-induced insulin resistance promotes Aβ peptide generation and amyloid plaque formation in the brain (66).

CCH induces memory deficits and facilitates Aβ generation in C57BL/6J mice, associated with BACE1 and δ-secretase up-regulation and neuronal apoptosis (67), which partially recapitulate AD-related pathologies. Moreover, BDNF mRNAs and protein are down-regulated in the hippocampus undergoing CCH as well as Aβ treatment (68). Therefore, BDNF is tightly correlated with both CCH and AD. We hypothesize that the artery occlusion may impact the profiles of pathologies and cognitive dysfunctions in $BDNF^{+/-}$ or $TrkB^{+/-}$ mice. It is possible that BDNF decrease in AD patients does not occur uniformly in the whole brain. $BDNF^{+/-}$ and $TrkB^{+/-}$ mice reduce the gene dose in the whole body to a half, which may not truly reflect the pathological process in AD. Nonetheless, these animal models partially recapitulate many aspects of the AD pathologies under the stress of risk factors including TBI. Beside TBI, HFD, and CCH, these mechanistic pathways are also responsive to other stressors related to the pathogenesis of AD, including but not limited to gender, cardiovascular disease, gastric intestinal tract inflammation, and so on. On the other hand, other crosstalk pathways, such as APOE4, cholesterol metabolism, and epigenetic regulation might be involved as well. Together, our study demonstrates that the C/EBPβ/δ-secretase pathway plays a critical role in mediating AD-associated pathologies. Since AD is a complex and multifactorial disorder, targeting one protease δ-secretase (AEP) that simultaneously truncates both APP and Tau, which provides the unprecedented advantage over the strategy pertinent to either APP or Tau alone. Identifying the pathological roles of δ-secretase in aging and AD onset will offer great promise to impact diagnosis, prevention, and treatment of neurodegenerative diseases.

Methods

Human Subjects. Autopsy brain tissue studies were performed with approval/exemption from the Emory University Institutional Review Board. Research brain tissues were provided by the University of Washington (UW) Alzheimer's Disease Research Center (ADRC) Neuropathology (NP) Core from well-characterized research subjects whose brains underwent extensive neuropathological characterization according to the latest guidelines. UW ADRC NP Core research autopsies include fresh tissue dissection when postmortem interval is less than 8 h, ensuring high-quality tissue for biochemical/molecular studies. Formalin-fixed, paraffin-embedded sections of midfrontal gyrus or dissected blocks of fresh midfrontal gyrus, flash frozen in liquid nitrogen at the time of autopsy, were provided from well-characterized AD and control subjects with no history of TBI with loss of consciousness (LOC) matched for age, sex, and postmortem interval with subjects with remote TBI with LOC. AD subjects were characterized as having neuropathologically confirmed AD (Braak neurofibrillary tangle stage V to VI, The Consortium to Establish a Registry for Alzheimer's Disease (CERAD) neuritic plaque cortical density score moderate/frequent) and controls with no/low AD pathology (Braak 0-III, CERAD none/sparse). Subjects were confirmed to have no Lewy body disease and no/low microvascular brain injury.

Animals. $BDNF^{f/f}$ mice were ordered from the Jackson Laboratory (Stock No: 004339). $TrkB^{f/f}$ mice (gifts from Dr. James O McNamara at Duke University, Durham, NC) were in a C57BL/6J background. Both of $TrkB^{f/f}$ and $BDNF^{f/f}$ mice were mated with Cre mice. Littermates without mutation were used as control group. Animal care and handling were performed according to the NIH animal care guidelines and Emory Medical School guidelines. The protocol was reviewed and approved by the Emory Institutional Animal Care and Use Committee. Male mice were used in the most of experiments; female mice were only used to test the gain of body weight with the treatment of HFD. Mice were randomized into different groups by using a random number table. Investigators were blinded to the group allocation during the animal experiments.

Procedures of TBI, HFD, and CCH. The experimental TBI method used in this study was performed as described previously with minor modification (33). The HFD model was followed the previous report (69). HFD (45% kcal) was obtained from Research Diet (catalog no. D12451). Mice at 2 mo old were fed with this diet for 3 mo. Regular chow food was feed as the control. The procedure of chronic cerebral hypoperfusion was described in the previous study (67).

Data Availability. All study data are included in the article and/or *SI Appendix*.

ACKNOWLEDGMENTS. We thank the University of Washington ADRC (NIH Grant No. P50AG005136) and the Kaiser Permanente Adult Changes in Thought Study (NIH Grant No. U01 AG006781) research subjects and their families for brain donation, a tremendous gift to science. We thank Ms. Allison Beller for coordination of tissue requests, subject selection, and tissue transfer and Ms. Kim Howard for histological support. This study was supported in part by the Rodent Behavioral Core, which is subsidized by the Emory University School of Medicine and is one of the Emory Integrated Core Facilities. Additional support was provided by the Viral Vector Core of the Emory Neuroscience National Institute of Neurological Disorders and Stroke (NINDS) Core Facilities (Grant No. P30NS055077). Further support was provided by the Georgia Clinical & Translational Science Alliance of the NIH under Award No. UL1TR002378. This work is supported by a grant from the NIH (RF1, Grant No. AG051538; RO1, Grant No. NS105982), and the ADRC center grant (P30, Grant No. AG066511) to K.Y., the Funds for International Cooperation and Exchange of the National Natural Science Foundation of China (NSFC) (Grant No. 81810001048), the National Basic Research Program of China (Grant No. 2016YFA0100800) to L.C., Shanghai Pujiang Program (Grant No. 19PJ1409200), and the National Natural Science Foundation of China (Grant No. 82071370) to Z.W. C.D.K. was supported by the Nancy and Buster Alvord Endowment.

1. D. J. Selkoe, Alzheimer's disease: Genes, proteins, and therapy. *Physiol. Rev.* **81**, 741–766 (2001).
2. P. Sullivan, D. Petitti, J. Barbaccia, Head trauma and age of onset of dementia of the Alzheimer type. *JAMA* **257**, 2289–2290 (1987).
3. Z. Guo *et al.*, Head injury and the risk of AD in the MIRAGE study. *Neurology* **54**, 1316–1323 (2000).
4. B. L. Plassman *et al.*, Documented head injury in early adulthood and risk of Alzheimer's disease and other dementias. *Neurology* **55**, 1158–1166 (2000).
5. J. T. Povlishock, C. W. Christman, The pathobiology of traumatically induced axonal injury in animals and humans: A review of current thoughts. *J. Neurotrauma* **12**, 555–564 (1995).
6. T. Bogoslovsky, J. Gill, A. Jeromin, C. Davis, R. Diaz-Arrastia, Fluid biomarkers of traumatic brain injury and intended context of use. *Diagnostics (Basel)* **6**, 37 (2016).
7. J. M. Anderson *et al.*, Abnormally phosphorylated tau is associated with neuronal and axonal loss in experimental autoimmune encephalomyelitis and multiple sclerosis. *Brain* **131**, 1736–1748 (2008).
8. J. Li, X. Y. Li, D. F. Feng, D. C. Pan, Biomarkers associated with diffuse traumatic axonal injury: Exploring pathogenesis, early diagnosis, and prognosis. *J. Trauma* **69**, 1610–1618 (2010).
9. J. H. Lee *et al.*, Therapeutic effects of pharmacologically induced hypothermia against traumatic brain injury in mice. *J. Neurotrauma* **31**, 1417–1430 (2014).

10. A. Ott *et al*., Diabetes mellitus and the risk of dementia: The Rotterdam Study. *Neurology* **53**, 1937–1942 (1999).
11. J. A. Luchsinger, M. X. Tang, S. Shea, R. Mayeux, Hyperinsulinemia and risk of Alzheimer disease. *Neurology* **63**, 1187–1192 (2004).
12. Y. Liu, F. Liu, I. Grundke-Iqbal, K. Iqbal, C. X. Gong, Deficient brain insulin signalling pathway in Alzheimer's disease and diabetes. *J. Pathol.* **225**, 54–62 (2011).
13. L. Frölich *et al*., Brain insulin and insulin receptors in aging and sporadic Alzheimer's disease. *J. Neural Transm. (Vienna)* **105**, 423–438 (1998).
14. E. Steen *et al*., Impaired insulin and insulin-like growth factor expression and signaling mechanisms in Alzheimer's disease–Is this type 3 diabetes? *J. Alzheimers Dis.* **7**, 63–80 (2005).
15. E. J. Rivera *et al*., Insulin and insulin-like growth factor expression and function deteriorate with progression of Alzheimer's disease: Link to brain reductions in acetylcholine. *J. Alzheimers Dis.* **8**, 247–268 (2005).
16. F. G. De Felice, Alzheimer's disease and insulin resistance: Translating basic science into clinical applications. *J. Clin. Invest.* **123**, 531–539 (2013).
17. J. C. de la Torre, Alzheimer disease as a vascular disorder: Nosological evidence. *Stroke* **33**, 1152–1162 (2002).
18. M. Altieri *et al*., Delayed poststroke dementia: A 4-year follow-up study. *Neurology* **62**, 2193–2197 (2004).
19. K. Farid, N. Caillat-Vigneron, I. Sibon, Is brain SPECT useful in degenerative dementia diagnosis? *J. Comput. Assist. Tomogr.* **35**, 1–3 (2011).
20. D. A. Snowdon *et al*., Brain infarction and the clinical expression of Alzheimer disease. The Nun Study. *JAMA* **277**, 813–817 (1997).
21. M. Bordeleau, A. ElAli, S. Rivest, Severe chronic cerebral hypoperfusion induces microglial dysfunction leading to memory loss in APPswe/PS1 mice. *Oncotarget* **7**, 11864–11880 (2016).
22. J. C. de la Torre *et al*., Hippocampal nitric oxide upregulation precedes memory loss and A beta 1-40 accumulation after chronic brain hypoperfusion in rats. *Neurol. Res.* **25**, 635–641 (2003).
23. A. Bartoletti *et al*., Heterozygous knock-out mice for brain-derived neurotrophic factor show a pathway-specific impairment of long-term potentiation but normal critical period for monocular deprivation. *J. Neurosci.* **22**, 10072–10077 (2002).
24. J. A. Gorski, S. R. Zeiler, S. Tamowski, K. R. Jones, Brain-derived neurotrophic factor is required for the maintenance of cortical dendrites. *J. Neurosci.* **23**, 6856–6865 (2003).
25. S. A. Heldt, L. Stanek, J. P. Chhatwal, K. J. Ressler, Hippocampus-specific deletion of BDNF in adult mice impairs spatial memory and extinction of aversive memories. *Mol. Psychiatry* **12**, 656–670 (2007).
26. H. S. Phillips *et al*., BDNF mRNA is decreased in the hippocampus of individuals with Alzheimer's disease. *Neuron* **7**, 695–702 (1991).
27. S. D. Ginsberg *et al*., Selective decline of neurotrophin and neurotrophin receptor genes within CA1 pyramidal neurons and hippocampus proper: Correlation with cognitive performance and neuropathology in mild cognitive impairment and Alzheimer's disease. *Hippocampus* **29**, 422–439 (2019).
28. M. G. Murer *et al*., An immunohistochemical study of the distribution of brain-derived neurotrophic factor in the adult human brain, with particular reference to Alzheimer's disease. *Neuroscience* **88**, 1015–1032 (1999).
29. S. Ando *et al*., Animal model of dementia induced by entorhinal synaptic damage and partial restoration of cognitive deficits by BDNF and carnitine. *J. Neurosci. Res.* **70**, 519–527 (2002).
30. S. Arancibia *et al*., Protective effect of BDNF against beta-amyloid induced neurotoxicity in vitro and in vivo in rats. *Neurobiol. Dis.* **31**, 316–326 (2008).
31. Z. Zhang *et al*., Delta-secretase cleaves amyloid precursor protein and regulates the pathogenesis in Alzheimer's disease. *Nat. Commun.* **6**, 8762 (2015).
32. Z. Zhang *et al*., Cleavage of tau by asparagine endopeptidase mediates the neurofibrillary pathology in Alzheimer's disease. *Nat. Med.* **20**, 1254–1262 (2014).
33. Z. Wu *et al*., Traumatic brain injury triggers APP and Tau cleavage by delta-secretase, mediating Alzheimer's disease pathology. *Prog. Neurobiol.* **185**, 101730 (2020).
34. Z. H. Wang *et al*., C/EBPβ regulates delta-secretase expression and mediates pathogenesis in mouse models of Alzheimer's disease. *Nat. Commun.* **9**, 1784 (2018).
35. A. Magalini *et al*., Role of IL-1 beta and corticosteroids in the regulation of the C/EBP-alpha, beta and delta genes in vivo. *Cytokine* **7**, 753–758 (1995).
36. A. Wedel, H. W. Ziegler-Heitbrock, The C/EBP family of transcription factors. *Immunobiology* **193**, 171–185 (1995).
37. M. S. Künzi, P. M. Pitha, Role of interferon-stimulated gene ISG-15 in the interferon-omega-mediated inhibition of human immunodeficiency virus replication. *J. Interferon Cytokine Res.* **16**, 919–927 (1996).
38. V. Poli, The role of C/EBP isoforms in the control of inflammatory and native immunity functions. *J. Biol. Chem.* **273**, 29279–29282 (1998).
39. H. Akiyama *et al*., Inflammation and Alzheimer's disease. *Neurobiol. Aging* **21**, 383–421 (2000).
40. Z. Wu *et al*., C/EBPbeta/delta-secretase signaling mediates Parkinson's disease pathogenesis via regulating transcription and proteolytic cleavage of alpha-synuclein and MAOB. *Mol. Psychiatry* **26**, 568–585 (2020).
41. R. Strohmeyer, J. Shelton, C. Lougheed, T. Breitkopf, CCAAT-enhancer binding protein-β expression and elevation in Alzheimer's disease and microglial cell cultures. *PLoS One* **9**, e86617 (2014).
42. Z. H. Wang *et al*., Deficiency in BDNF/TrkB neurotrophic activity stimulates δ-secretase by upregulating C/EBPβ in Alzheimer's disease. *Cell Rep.* **28**, 655–669.e5 (2019).
43. G. S. Meneilly, D. Tessier, Diabetes in elderly adults. *J. Gerontol. A Biol. Sci. Med. Sci.* **56**, M5–M13 (2001).
44. I. Ferrer *et al*., BDNF and full-length and truncated TrkB expression in Alzheimer disease. Implications in therapeutic strategies. *J. Neuropathol. Exp. Neurol.* **58**, 729–739 (1999).
45. D. J. Selkoe, Alzheimer's disease is a synaptic failure. *Science* **298**, 789–791 (2002).
46. R. D. Terry *et al*., Physical basis of cognitive alterations in Alzheimer's disease: Synapse loss is the major correlate of cognitive impairment. *Ann. Neurol.* **30**, 572–580 (1991).
47. M. Vandal *et al*., Age-dependent impairment of glucose tolerance in the 3xTg-AD mouse model of Alzheimer's disease. *FASEB J.* **29**, 4273–4284 (2015).
48. C. L. Masters *et al*., Alzheimer's disease. *Nat. Rev. Dis. Primers* **1**, 15056 (2015).
49. S. Chakrabarti *et al*., Metabolic risk factors of sporadic Alzheimer's disease: Implications in the pathology, pathogenesis and treatment. *Aging Dis.* **6**, 282–299 (2015).
50. G. A. Elder, M. A. Gama Sosa, R. De Gasperi, Transgenic mouse models of Alzheimer's disease. *Mt. Sinai J. Med.* **77**, 69–81 (2010).
51. M. P. Mattson, Pathways towards and away from Alzheimer's disease. *Nature* **430**, 631–639 (2004).
52. A. Paquin, F. Barnabé-Heider, R. Kageyama, F. D. Miller, CCAAT/enhancer-binding protein phosphorylation biases cortical precursors to generate neurons rather than astrocytes in vivo. *J. Neurosci.* **25**, 10747–10758 (2005).
53. Y. Soga, R. Yamanaka, K. Nishino, R. Tanaka, CCAAT/enhancer binding proteins are expressed in the gerbil hippocampus after transient forebrain ischemia. *Neurosci. Lett.* **337**, 106–110 (2003).
54. M. Samuelsson, V. Ramberg, K. Iverfeldt, Alzheimer amyloid-beta peptides block the activation of C/EBPbeta and C/EBPdelta in glial cells. *Biochem. Biophys. Res. Commun.* **370**, 619–622 (2008).
55. S. M. Taubenfeld, M. H. Milekic, B. Monti, C. M. Alberini, The consolidation of new but not reactivated memory requires hippocampal C/EBPbeta. *Nat. Neurosci.* **4**, 813–818 (2001).
56. W. J. Lukiw, Gene expression profiling in fetal, aged, and alzheimer hippocampus: A continuum of stress-related signaling. *Neurochem. Res.* **29**, 1287–1297 (2004).
57. R. Li, R. Strohmeyer, Z. Liang, L. F. Lue, J. Rogers, CCAAT/enhancer binding protein delta (C/EBPdelta) expression and elevation in Alzheimer's disease. *Neurobiol. Aging* **25**, 991–999 (2004).
58. A. M. Calella *et al*., Neurotrophin/Trk receptor signaling mediates C/EBPalpha, -beta and NeuroD recruitment to immediate-early gene promoters in neuronal cells and requires C/EBPs to induce immediate-early gene transcription. *Neural Dev.* **2**, 4 (2007).
59. D. Bambah-Mukku, A. Travaglia, D. Y. Chen, G. Pollonini, C. M. Alberini, A positive autoregulatory BDNF feedback loop via C/EBPβ mediates hippocampal memory consolidation. *J. Neurosci.* **34**, 12547–12559 (2014).
60. K. Marosi, M. P. Mattson, BDNF mediates adaptive brain and body responses to energetic challenges. *Trends Endocrinol. Metab.* **25**, 89–98 (2014).
61. J. Gray *et al*., Hyperphagia, severe obesity, impaired cognitive function, and hyperactivity associated with functional loss of one copy of the brain-derived neurotrophic factor (BDNF) gene. *Diabetes* **55**, 3366–3371 (2006).
62. G. S. Yeo *et al*., A de novo mutation affecting human TrkB associated with severe obesity and developmental delay. *Nat. Neurosci.* **7**, 1187–1189 (2004).
63. S. G. Kernie, D. J. Liebl, L. F. Parada, BDNF regulates eating behavior and locomotor activity in mice. *EMBO J.* **19**, 1290–1300 (2000).
64. T. Nakagawa *et al*., Brain-derived neurotrophic factor regulates glucose metabolism by modulating energy balance in diabetic mice. *Diabetes* **49**, 436–444 (2000).
65. C. W. Cotman, The role of neurotrophins in brain aging: A perspective in honor of regino Perez-Polo. *Neurochem. Res.* **30**, 877–881 (2005).
66. L. Ho *et al*., Diet-induced insulin resistance promotes amyloidosis in a transgenic mouse model of Alzheimer's disease. *FASEB J.* **18**, 902–904 (2004).
67. L. Wang *et al*., Chronic cerebral hypoperfusion induces memory deficits and facilitates Aβ generation in C57BL/6J mice. *Exp. Neurol.* **283**, 353–364 (2016).
68. Q. Li, J. Cui, C. Fang, X. Zhang, L. Li, S-adenosylmethionine administration attenuates low brain-derived neurotrophic factor expression induced by chronic cerebrovascular hypoperfusion or beta amyloid treatment. *Neurosci. Bull.* **32**, 153–161 (2016).
69. C. B. Chan *et al*., Activation of muscular TrkB by its small molecular agonist 7,8-dihydroxyflavone sex-dependently regulates energy metabolism in diet-induced obese mice. *Chem. Biol.* **22**, 355–368 (2015).
70. Z. Wu, X. Liu, L. Cheng, K. Ye, Delta-secretase triggers Alzheimer's disease pathologies in wild-type hAPP/hMAPT double transgenic mice. *Cell Death Dis.* **11**, 1058 (2020).
71. T. Bussière *et al*., Morphological characterization of Thioflavin-S-positive amyloid plaques in transgenic Alzheimer mice and effect of passive Abeta immunotherapy on their clearance. *Am. J. Pathol.* **165**, 987–995 (2004).
72. W. D. Dupont, W. D. Plummer Jr, Power and sample size calculations. A review and computer program. *Control. Clin. Trials* **11**, 116–128 (1990).